

Electrochemical and Quantum Chemical Study of Albendazole as Corrosion Inhibitor for Mild Steel in Hydrochloric Acid Solution

I. Ahamad¹, R. Prasad², Eno E. Ebenso³, M.A. Quraishi^{1,*}

¹ Department of Applied Chemistry, Institute of Technology, Banaras Hindu University, Varanasi 221005 (India)

² Department of Chemistry, SGB Amravati University, Amravati 444 602, India

³ Department of Chemistry, School of Mathematical and Physical Sciences, North-West University (Mafikeng Campus), Private Bag X2046, Mmabatho 2735, South Africa

*E-mail: maquraishi@rediffmail.com; maquraishi.apc@itbhu.ac.in

Received: 12 February 2012 / Accepted: 3 March 2012 / Published: 1 April 2012

Inhibition effect of Albendazole on the mild steel corrosion in molar hydrochloric acid was investigated using weight loss, electrochemical impedance spectroscopy (EIS) and polarization techniques. The results show that Albendazole is an effective inhibitor for mild steel corrosion in 1 M HCl solutions and inhibition efficiency is >90% at inhibitor concentration of 0.4 mM. Adsorption of the inhibitor on the mild steel surface followed Langmuir adsorption isotherm. The value of free energy of adsorption ($\Delta G_{\text{ads}}^{\circ}$) indicated that adsorption of Albendazole molecule is a spontaneous process and it adsorbs chemically as well as physically. Polarization studies showed that albendazole is a mixed-type inhibitor. Quantum chemical calculations were performed on Albendazole using unrestricted Kohn-Sham formalism at density functional theory (DFT) level based on self-consistent field (SCF) method with the 6-31**G (d,p) basis set for all atoms by Gaussian 03W program. The different quantum chemical properties were calculated and discussed.

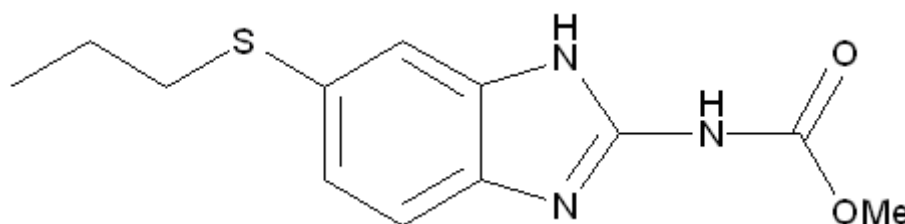
Keywords: Electrochemical; Quantum chemical calculation; Corrosion inhibition; Acid solution; Adsorption

1. INTRODUCTION

Evaluation of corrosion inhibitors for mild steel in acidic media is important for both theoretical as well as industrial point of views. Acid solutions are generally used for the removal of rust and scale in industrial processes. Hydrochloric acid is widely used in the pickling, cleaning and descaling of steel and ferrous alloys [1]. Most of the effective corrosion inhibitors are organic

compounds containing nitrogen, oxygen, sulphur, aromatic rings and π -electrons in their structures [2, 3]. The effectiveness of these organic compounds as corrosion inhibitors has been interpreted in terms of their molecular structure, molecular size, molecular mass, presence of hetero-atoms and adsorptive tendencies [4]. The first stage in the action mechanism of these compounds in acid media is their adsorption on the metal surface [5]. The various inhibition mechanisms are considered regarding different situations created by changing various factors such as medium and inhibitor in the system metal/acid medium/inhibitor [6]. The interactions between the inhibitor molecules and the metal surface can be explained and understood in details by theoretical approaches. Therefore, recently a trend and an increasing attention were seen on the involvement of these theoretical approaches in corrosion studies [7-9]. Quantum chemical calculations have been used recently to explain the mechanism of corrosion inhibition [10, 11].

The strict environmental legislation has restricted use of most of the commercial inhibitors. This has led to the development of drugs as corrosion inhibitors in recent years. In continuation of our work on the development of drugs as corrosion inhibitors [12-15], the present work describes the investigation of inhibitive action of Albendazole on corrosion of the mild steel in molar hydrochloric acid solutions using weight loss, electrochemical impedance spectroscopy (EIS), potentiodynamic polarization, theoretical calculations and scanning electron microscopy (SEM). The choice of this compound was based on molecular structure considerations. The Albendazole molecule is made up of a benzimidazole ring of planar structure with delocalized pi electrons (aromaticity), a propylthio group and a methyl carbamate group ($-\text{NHCOOCH}_3$). These structural features favour the interaction of Albendazole with metal. Furthermore, the Albendazole molecule is big enough (molecular weight = 265) and planar to block large surface area (due to adsorption) of the mild steel. In view of these favorable characteristics, Albendazole was chosen for the present work. The IUPAC name and structure of Albendazole is given in Figure 1.



Methyl [6-(propylthio)-1*H*-benzimidazol-2-yl]carbamate (Albendazole)

Figure 1. The chemical structure and IUPAC name of Albendazole.

2. EXPERIMENTAL DETAILS

Mild steel specimens (having compositions 0.076 % C; 0.192 % Mn; 0.050 % Cr; 0.026 % Si; 0.012 % P; 0.135 % Cu; 0.023 % Al; 0.05 % Ni and remainder being iron) of size 2.5 cm \times 2.0 cm \times 0.025 cm were used for weight loss measurements and of size 7.5 cm \times 1.0 cm \times 0.025 cm with 1.0

cm² exposed surface area (isolated with commercially available epoxy resin) for electrochemical measurements. Prior to all experiments, the mild steel specimens were cleaned and prepared as per ASTM standard G1-03 [16].

The studied drug is available under the brand name Albendazole manufactured by Cipla Ltd. Central Mumbai, Mumbai (India). Stock solution of drug was made in 10:1 ratio of water: methanol mixture to ensure solubility. This stock solution was used for all experimental purposes. We have added the same quantity of methanol to free acid solution to avoid the contribution of methanol. All solutions were freshly prepared from analytical grade chemical reagents using double distilled water.

Weight loss measurements were performed on the mild steel specimens in 1 M HCl solution (100 mL) with and without addition of different concentrations of inhibitor [17]. The duration of the immersion was 3 h at the temperature range from 308 to 338 K. After immersion, the surface of the specimen was cleaned by double distilled water followed rinsing with acetone and then specimen was weighed in order to calculate inhibition efficiency ($E\%$) and the corrosion rate (C_R). For each experiment, a freshly prepared solution was used and the solution temperature was thermostatically controlled at a desired value. The inhibition efficiency ($E\%$) and corrosion rate (C_R , mm year⁻¹) were calculated as described elsewhere [1].

All electrochemical measurements were performed using a GAMRY PCI 4/300 electrochemical work station based on ESA 400. Gamry applications include EIS 300 (for EIS measurements) and DC 105 software (for corrosion) and Echem Analyst (5.5 V.) software for data fitting. All electrochemical experiments were performed in a Gamry three electrodes electrochemical cell under atmospheric condition with a platinum counter electrode and a saturated calomel electrode (SCE) as the reference electrode. The working electrode the mild steel (7.5 cm long stem) with the exposed surface of 1 cm² was immersed into aggressive solutions with and without inhibitor, and measurements were initiated about 30 min after the working electrode was immersed in solution to stabilize the steady state potential. EIS measurements were performed at corrosion potentials (E_{corr}) over a frequency range of 10⁵ Hz to 10⁻² Hz with an AC signal amplitude perturbation of 10 mV peak to peak. Potentiodynamic polarization studies were performed with a scan rate of 1 mV s⁻¹ in the potential range from 250 mV below the corrosion potential to 250 mV above the corrosion potential. All potentials were recorded with respect to the SCE. The values of inhibition efficiency from charge transfer resistance and corrosion current density were calculated using equations (1) and (2), respectively:

$$E\% = \frac{R_{t,i} - R_{t,0}}{R_{t,i}} \times 100 \quad (1)$$

where $R_{t,i}$ and $R_{t,0}$ are charge transfer resistances in the presence and absence of inhibitor, respectively; and

$$E\% = \frac{I_{\text{corr}} - I_{\text{corr}(i)}}{I_{\text{corr}}} \times 100 \quad (2)$$

where I_{corr} and $I_{\text{corr(i)}}$ are corrosion current densities obtained in the absence and presence of inhibitor, respectively.

Quantum chemical calculations for the molecular parameters related to albendazole were calculated using unrestricted Kohn-Sham formalism at density functional theory (DFT) level. For all DFT calculations, the Perdew–Burke–Ernzerhof (PBE 1) functional [18] was used. We have chosen PBE1 functional because it has many times proved its efficiency on a wide range of compounds, and it generally provides accurate results on ground and excited-state properties, including charge-transfer transitions [9, 19]. The split valence 6-31G** basis sets were used for all atoms and quantum chemical calculations were performed with the help of Gaussian 03 package [20]. We have performed all calculations in gas phase.

3. RESULTS AND DISCUSSION

3.1. Weight loss measurements

Corrosion parameters obtained from weight loss measurements for the mild steel in 1 M HCl solution in the absence and presence of different concentrations of Albendazole are summarized in Table 1. It can be observed that $E\%$ increases as inhibitor concentration increased from 0.04 to 0.4 mM (Table 1). This behavior is the result of increased adsorption and increased coverage of inhibitor on the mild steel surface with increase in the inhibitor concentration.

Table 1. Corrosion rates of mild steel in 1 M HCl and inhibition efficiency for different concentrations of Albendazole obtained from weight loss measurements

Concentration (mM)	weight loss ($\text{mg cm}^{-2} \text{ h}^{-1}$)	E (%)	C_R (mm year^{-1})
1 M HCl	7	–	78
0.04	3.4	51	38
0.1	1	86	11
0.2	0.5	93	6
0.3	0.4	95	4
0.4	0.3	96	3

The effect of temperature on the inhibition performance of albendazole for mild steel in molar hydrochloric acid solution in the absence and presence of 0.4 mM at temperature ranging from 308 to 338 K was obtained by weight loss measurements. The results are given in Figure 2. This figure shows that inhibition efficiency decreases with increasing the solution temperature from 308 to 338 K. This can be attributed to increased rate of desorption of inhibitor molecules from the surface of mild steel with increasing temperature. These results confirmed that albendazole acts as a good inhibitor for mild steel in molar hydrochloric acid solution in the range of temperature studied.

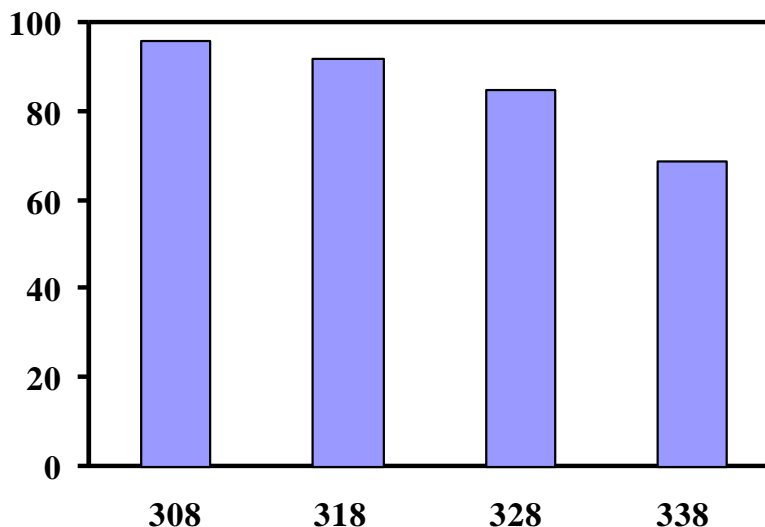


Figure 2. Effect of temperature (T) on $E\%$ for the mild steel in 1 M HCl in the presence of 0.4 mM Albendazole.

In order to have better understanding of thermodynamic properties of the mild steel corrosion processes in the presence of albendazole, a detailed study on corrosion behaviour of mild steel was carried out at a temperature range 308 to 338 K using weight loss technique. The corrosion reaction can be regarded as an Arrhenius-type process, the rate of which is given by:

$$C_R = \lambda \exp\left(-\frac{E_a}{RT}\right) \tag{3}$$

where E_a is the activation energy for corrosion of the mild steel in 1 M HCl solution, R the general gas constant, λ the Arrhenius pre-exponential factor and T the absolute temperature. A plot of the logarithm of the corrosion rate (mm year^{-1}) of mild steel obtained from weight loss measurements vs. $1/T$ gave a straight line as shown in Figure 3a. The values of E_a and λ obtained from the slope and intercept, respectively of this line (Figure 3a) are presented in Table 2.

Table 2. Activation parameters E_a , ΔH^* and ΔS^* for the mild steel dissolution in 1 M HCl in the absence and the presence of 0.4 mM Albendazole

Inhibitor	E_a (kJ mol ⁻¹)	λ	ΔH^* (kJ mol ⁻¹)	ΔS^* (kJ mol ⁻¹)	Temperature (K)	K_{ads} ($\times 10^4 \text{ M}^{-1}$)	$\Delta G^\circ_{\text{ads}}$ (kJ mol ⁻¹)
1 M HCl	29	7×10^6	27	-123		-	-
Albendazole	89	2×10^{15}	86	44	308	7	-39
					318	3	-38
					328	2	-37
					338	0.6	-36

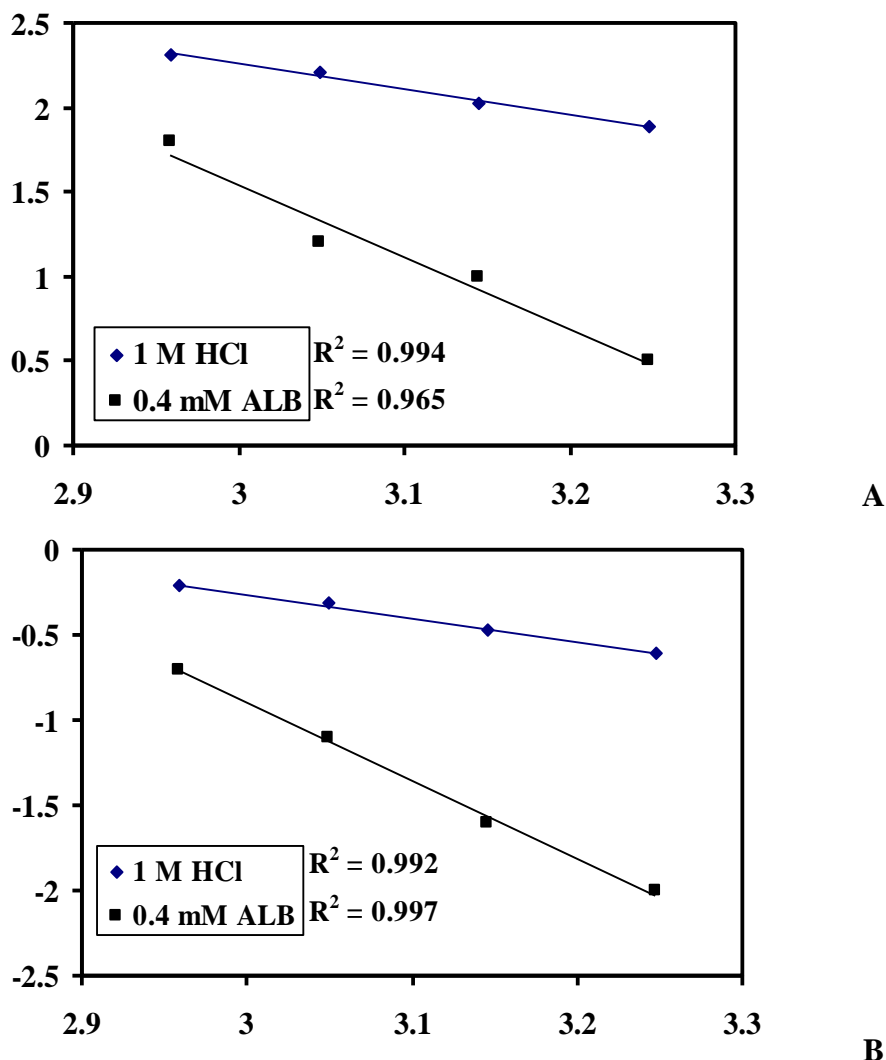


Figure 3. Arrhenius plots of: (a) $\log C_R$ vs. $1,000/T$; (b) $\log (C_R/T)$ vs. $1,000/T$ for the mild steel in 1 M HCl solution in the absence and presence of 0.4 mM Albendazole.

An alternative formula of the Arrhenius equation is the transition state equation:

$$C_R = \frac{RT}{Nh} \exp\left(-\frac{\Delta H^*}{RT}\right) \exp\left(\frac{\Delta S^*}{R}\right) \quad (4)$$

where N is the Avogadro's number, h the Planck's constant, ΔH^* the enthalpy of activation and ΔS^* the entropy of activation. Figure 3b showed a plot of $\log (C_R/T)$ versus $1/T$ giving a straight line with a slope of $(-\Delta H^* / 2.303 R)$ and an intercept of $\log (R / Nh + \Delta S^* / 2.303 R)$ from which the values of ΔH^* and ΔS^* were calculated and given in Table 2. The data in Table 2 reveal that the values of thermodynamic activation functions (E_a and ΔH^*) for corrosion of the mild steel in 1 M HCl solution in the presence of the inhibitor are higher than those in the free acid solution. Higher values of E_a and ΔH^* in the presence of inhibitor indicate more energy is required for dissolution of the mild steel in 1 M HCl in presence of albendazole. Similar results were reported by other authors [21, 22].

Higher value of activation energy for the mild steel dissolution in inhibited solution indicates a strong inhibitive action for the studied compounds by increasing the energy barrier for the corrosion process. Szauer and Brandt explained [23] that the increase in activation energy can be attributed to an appreciable decrease in the adsorption of the inhibitor on the mild steel surface with increase in temperature.

The pre-exponential factor λ in the Arrhenius equation (Eq. 3) for corrosion process, heterogeneous reaction, is related to the number of active centers. These active centers have different energy if energetic surface heterogeneity is assumed. In present case $E_{a,inh} > E_{a,HCl}$ that is the inhibitor is adsorbed on the most active adsorption sites (having the lowest energy) and corrosion process occurred predominantly on the active sites of higher energy. Values of E_a and λ obtained in the presence of albendazole are higher than those obtained in free acid solutions which mean that the presence of albendazole results in high number of active centres remain uncovered with the inhibitor. In literature, some authors [22, 24] have shown that for most corrosion reactions, the tendency of variation in pre-exponential factor is similar to that in activation energy; for the present system, similar phenomenon has been observed (Table 2).

Inspection of Table 2 showed that value of enthalpy of activation is positive and higher in the presence of inhibitor indicating that mild steel dissolution process is endothermic, emphasizing mild steel dissolution increases with increase in temperature. It is also observed that $E_a > \Delta H^*$ by a value which approximately equal to RT . From the thermodynamic and kinetic point of view, the unimolecular reaction is characterized by following equation [25]:

$$E_a - \Delta H^* = RT \quad (5)$$

Thus, mild steel sample corrodes in 1.0 M HCl solutions either in absence or presence of different concentrations of the studied inhibitors by a unimolecular reaction.

The entropy of activation ΔS^* in the absence of the inhibitor is large and negative, while in the presence of inhibitor it is positive ($44 \text{ J K}^{-1} \text{ mol}^{-1}$). This indicates that the activated complex in the rate determining step represents dissociation rather than association step, meaning that, a increase in disordering takes place on going from reactants to the activated complex.

The standard free energy of adsorption (ΔG_{ads}°) at different temperatures was calculated from the equation:

$$\Delta G_{ads}^\circ = -2.303RT \log(55.55K_{ads}) \quad (6)$$

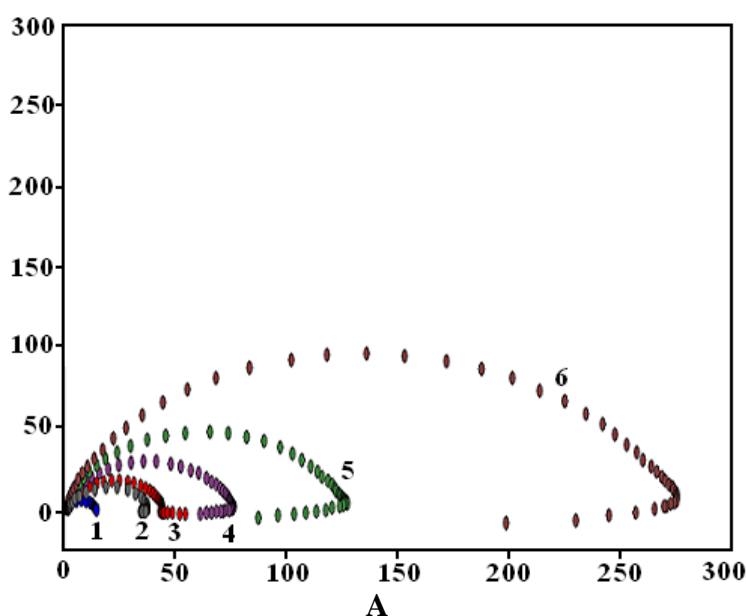
where the value 55.5 is the concentration of water in solution expressed in M [26] and K_{ads} is equilibrium adsorption constant.

Table 2 showed the values of adsorption equilibrium constant and standard free energy for the mild steel in 1 M HCl solution in the presence of 0.4 mM Albendazole. The negative value of ΔG_{ads}° suggested that the adsorption of inhibitor molecules onto the mild steel surface is a spontaneous process [27]. The large value of adsorption equilibrium constant also suggests the spontaneity of the

adsorption process and stability of the adsorbed layer on the mild steel surface. Generally, the value of the $\Delta G^{\circ}_{\text{ads}}$ of -40 kJ mol^{-1} is usually accepted as a threshold value between chemisorption and physisorption. The values of $\Delta G^{\circ}_{\text{ads}}$ up to -20 kJ mol^{-1} or higher are consistent with the electrostatic interaction between the charged molecules and the charged metal (physical adsorption) while those more negative than -40 kJ mol^{-1} involve sharing or transfer of electrons from the inhibitor molecules to the metal surface to form a coordinate type of bond (chemisorption) [28, 29]. The value of standard free energy of adsorption ($\Delta G^{\circ}_{\text{ads}}$) calculated in the presence of albendazole was -39 kJ mol^{-1} at 308 K. This indicates that the adsorption of inhibitor molecules is not merely physisorption or chemisorption but obeying a comprehensive adsorption (physical and chemical adsorption). Thus adsorption mechanism of the Albendazole on the mild steel surface in 1 M HCl solution involves comprehensive adsorption mechanism. This is further supported by values of $\Delta G^{\circ}_{\text{ads}}$ at different temperatures (Table 2). Moreover, higher value of K_{ads} favours adsorption process. In present case, K_{ads} values are higher (varies between $7 \times 10^4 \text{ M}^{-1}$ and $0.6 \times 10^4 \text{ M}^{-1}$ at temperatures from 308 to 338 K) suggesting strong interaction of inhibitor molecules with metal surface. The strong adsorption of inhibitor molecules on the mild steel surface can be attributed to donor acceptor interaction between electron density of hetero-atoms and aromatic ring of inhibitor and vacant d-orbitals of iron atoms at the metal surface [30].

3.2. Electrochemical impedance spectroscopy (EIS) studies

Results obtained from EIS measurements for mild steel in 1 M HCl solution in the absence and presence of different concentrations of albendazole were presented in the form of Nyquist (Figure 4a) and Bode plots (Figure 4b). The plots showed a depressed capacitive loop which arises from the time constant of the electrical double layer and charge transfer resistance. The impedance of the inhibited mild steel increases with increase in the inhibitor concentration and consequently the inhibition efficiency increased.



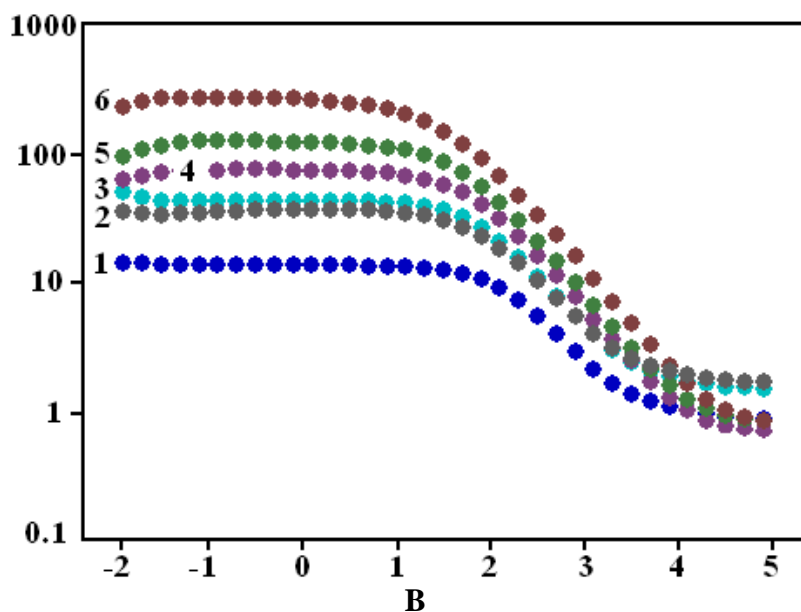


Figure 4. (a) Nyquist plots and (b) Bode-impedance plots for the mild steel in 1 M HCl containing different concentrations of Albendazole.

A depressed semicircle is mostly referred to as frequency dispersion which could be attributed to different physical phenomena such as roughness and inhomogeneities of the solid surfaces, impurities, grain boundaries and distribution of the surface active sites [31]. Inhibitor molecules get adsorbed on the mild steel/acid solution interface and thereby produce a barrier for the metal to diffuse out to the bulk and this barrier increases with increasing the inhibitor concentration.

The equivalent circuit used to fit the experimental data is presented in Figure 5, which has been used previously to model the mild steel/acid interface [32, 33]. This equivalent circuit consists solution resistance R_s and CPE Q ($n = 1, Q = C_{dl}$) in parallel to the series resistors R_t and an inductor (L). The charge transfer resistance (R_t) must be corresponding to the resistance between the metal and OHP (outer Helmholtz plane) and can be calculated from the difference in impedance at lower and higher frequencies.

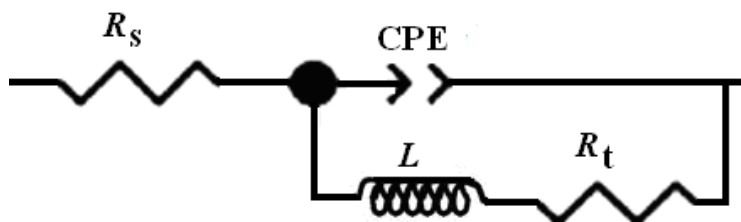


Figure 5. The electrochemical equivalent circuit used to fit the impedance results.

Mathematically, amplitude of CPE is given by the relation:

$$Z_{CPE} = Q^{-1}(j\omega)^{-n} \tag{7}$$

where Q is the magnitude of the CPE, j is the imaginary unit, ω is the angular frequency ($\omega = 2\pi f$, the frequency in Hz), and n is the phase shift which gives details about the degree of surface inhomogeneity. When $n = 1$, this is the same equation as that for the impedance of a capacitor, where $Q = C_{dl}$. In fact, when n is close to 1, the CPE resembles a capacitor, but the phase angle is not 90° . It is constant and somewhat less than 90° at all frequencies.

The term double layer capacitance is still often used in the evaluation of electrochemical impedance results to characterize the double layer which is believed to be formed at the metal/solution interface of systems displaying non-ideal capacitive behavior. For providing simple comparison between the capacitive behaviors of different corrosion systems, the values of Q were converted to C_{dl} using the relation [34]:

$$C_{dl} = Q(\omega_{max})^{n-1} \tag{8}$$

here, ω_{max} represents the frequency at which the imaginary component reaches a maximum. It is the frequency at which the real part (Z_r) is midway between the low and high frequency x-axis intercepts.

Various electrochemical impedance parameters obtained by fitting the Nyquist plots are listed in Table 3.

Table 3. Electrochemical impedance properties for mild steel in 1 M HCl in the absence and presence of Albendazole at different concentrations

Concentration (mM)	R_s ($\Omega \text{ cm}^2$)	R_{ct} ($\Omega \text{ cm}^2$)	L (10^{-3} H)	Q ($10^{-6} \Omega^{-1} \text{ s}^n \text{ cm}^{-2}$)	n	C_{dl} ($\mu\text{F cm}^{-2}$)	E (%)	d (10^{-5} cm)
1 M HCl	0.84	12.6	8.9	832.8	0.782	139.3	-	6.4
0.04	0.71	33.3	13.3	165.2	0.835	59.3	62	14.9
0.1	0.52	41.6	15.8	125.4	0.861	52.9	69	16.7
0.2	0.6	72.3	18.4	84.4	0.86	36.5	83	24.2
0.3	0.75	117.6	39.6	63.7	0.867	30.7	89	28.8
0.4	0.64	260	70.4	48.5	0.845	22.2	95	39.9

It is clear that addition of albendazole into the corrosive solution caused an increase in the charge transfer resistance (R_t) and a decrease in the double layer capacitance (C_{dl}) which can be given as [35]:

$$C_{dl} = \frac{\epsilon\epsilon_0 A}{d} \tag{9}$$

where ϵ_0 is the vacuum dielectric constant, ϵ is the local dielectric constant, d is the thickness of the double layer, and A is the surface area of the electrode. It is obvious that a decrease in C_{dl} can happen if the inhibitor molecules (low dielectric constant) replace the adsorbed water molecules (high dielectric constant) on the mild steel surface. The capacitance is inversely proportional to the thickness of the double layer.

Thus, decrease in the C_{dl} values could be attributed to the adsorption of albendazole on the metal surface. Decrease in the capacitance, which can result from a decrease in the local dielectric constant and/or an increase in the thickness of the electrical double layer (Table 3), strongly suggests that the inhibitor molecules adsorbed at the metal/solution interface. In the absence and in the presence of inhibitor, phase shift value remained more or less identical; this indicates that the charge transfer process controls the dissolution mechanism [36] of mild steel in molar hydrochloric acid solution in the absence and in the presence of Albendazole.

3.3. Potentiodynamic polarization studies

The results obtained from potentiodynamic polarization measurements for the mild steel in molar hydrochloric acid solution in the absence and presence of different concentrations of Albendazole are presented in Figure 6. It can be seen that both the cathodic and anodic reactions were suppressed in the presence of albendazole, which suggested that albendazole reduced both the anodic dissolution and the cathodic hydrogen evolution reactions.

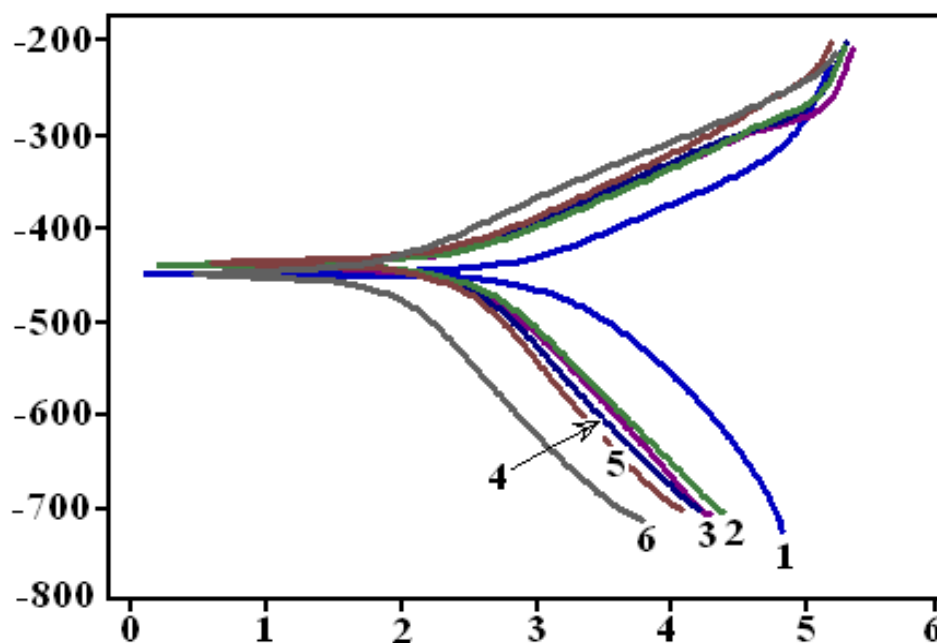


Figure 6. Tafel polarization curves for the corrosion of mild steel in 1 M HCl in the absence and presence of different concentrations of Albendazole.

Table 4. Polarization parameters for mild steel in 1 M HCl in the absence and presence of Albendazole at different concentrations

Concentration (mM)	E_{corr} (mV / SCE)	I_{corr} ($\mu\text{A cm}^{-2}$)	b_c (mV dec ⁻¹)	b_a (mV dec ⁻¹)	E (%)
1 M HCl	-448	1100	98	66	-
0.04	-437	445	40	34	60
0.1	-438	406	100	72	63
0.2	-437	183	110	64	83
0.3	-439	128	112	71	88
0.4	-449	97	90	56	91

Electrochemical corrosion parameters i.e. corrosion potential (E_{corr}), cathodic and anodic Tafel slopes (b_c , b_a), and corrosion current density (I_{corr}) obtained from the Tafel extrapolation of the polarization curves along with inhibition efficiency are given in Table 4. These values were calculated from the Tafel fit routine provided by Gamry Echem Analyst software, this routine uses a non-linear chi squared minimization to fit the data to the Stern-Geary equation.

The results in Table 4 showed that the inhibition efficiency increased, while the corrosion current density decreased with increasing concentration of Albendazole. This could be explained on the basis of adsorption of albendazole on the mild steel surface and the adsorption process enhanced with increasing inhibitor concentration. The values of corrosion potential (E_{corr}) were found to be almost identical at all albendazole concentrations, indicating that it acts as mixed-type inhibitor [13]. From Table 4, it is clear that the values of both anodic and cathodic Tafel slope constants were more or less constant suggesting that presence of Albendazole molecules does not alter the mechanism of corrosion in HCl environment.

3.4. Adsorption isotherm

Adsorption of organic inhibitor molecules is often a displacement reaction involving removal of adsorbed water molecules from the metal surface:



where x is the size ratio that is, the number of water molecules replaced by one organic inhibitor molecule. In order to understand the mechanism of corrosion inhibition, adsorption behavior of the organic compounds at mild steel/acid solution interface must be known. Basic information dealing with interaction between inhibitor molecules and the metal surface can be provided by adsorption isotherms.

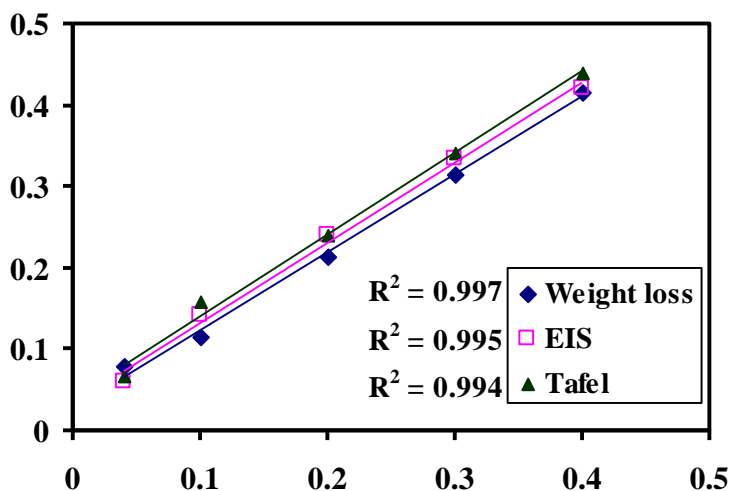


Figure 7. Langmuir adsorption isotherm plots for the adsorption of the Albendazole on the mild steel surface in 1 M HCl solution by using surface coverage values calculated by different techniques at 308 K.

The values of degree of surface coverage (θ) for the inhibitor were obtained from weight loss, EIS and potentiodynamic data. The data obtained from these techniques have been tested with several adsorption isotherms (such as Frumkin, Langmuir, Temkin, Freundlich, Bockris–Swinkels and Flory–Huggins isotherms). The Langmuir adsorption isotherm was found to provide the best description of the adsorption behavior of albendazole at the mild steel/acid solutions interface. The plot of C_{inh} / θ versus C_{inh} yields straight lines (Figure 7) with regression coefficients (R^2) almost equal to 1. This suggested that albendazole in present study obeyed the Langmuir adsorption isotherm model which is given as:

$$\frac{C_{inh}}{\theta} = \frac{1}{K_{ads}} + C_{inh} \quad (11)$$

where C_{inh} is the molar concentration of inhibitor.

3.5. Quantum chemical calculations

Computational methods have a potential application towards the design and development of organic corrosion inhibitors in the field of corrosion [37, 38]. The major thrust of quantum chemical research is to understand and explain the functions of these organic compounds in molecular terms. In order to support experimental data obtained from different techniques viz., weight loss and electrochemical, quantum chemical calculations were conducted in order to provide molecular-level understanding of the observed experimental behaviour.

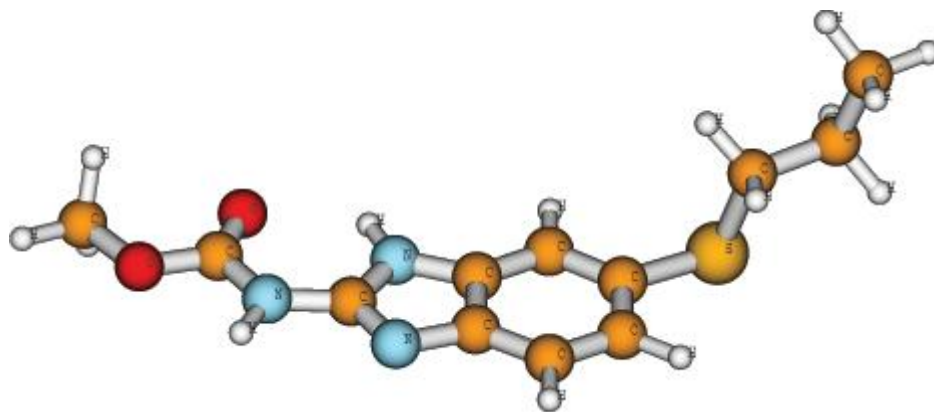


Figure 8. Optimized structure of Albendazole.

The optimized equilibrium structure of Albendazole is shown in Figure 8. Some computed molecular parameters such as energy of the highest occupied molecular orbital (E_{HOMO}), energy of the lowest unoccupied molecular orbital (E_{LUMO}), the HOMO-LUMO energy gap ($\Delta E_{\text{L-H}}$) and molecular band gap (ΔE_{MBG}) are presented in Table 5.

Table 5. Computed quantum chemical properties for Albendazole

E_{HOMO}	E_{LUMO}	$\Delta E_{\text{L-H}}$	ΔE_{MBG}	E
(eV)	(eV)	(eV)	(eV)	(%)
-5.2	-0.5	4.7	3.4	96

These quantum chemical parameters were obtained after geometric optimization with respect to the all nuclear coordinates using Kohn-Sham approach at DFT level. The molecular band gap was computed as the first vertical electronic excitation energy from the ground state using the time-dependent density functional theory (TD-DFT) approach as implemented in Gaussian 03.

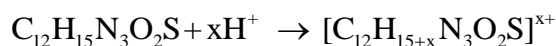
Frontier orbital theory is useful in predicting adsorption centers of the inhibitor molecules responsible for the interaction with surface metal atoms [10, 39]. Terms involving the frontier MO could provide dominative contribution, because of the inverse dependence of stabilization energy on orbital energy difference [39]. Moreover, the gap between the HOMO and LUMO energy levels of the molecules was another important factor that could be considered. Reportedly, excellent corrosion inhibitors are usually those organic compounds who not only offer electrons to unoccupied orbital of the metal, but also accept free electrons from the metal [39, 40].

It is understood from literature that higher the E_{HOMO} of the inhibitor, greater the ease of offering electrons to unoccupied d orbital of the metal, and the higher corrosion inhibition efficiency for iron in hydrochloric acid solutions; in addition, as the LUMO–HOMO energy gap ($\Delta E_{\text{L-H}}$) decreased, interactions between the reacting species become stronger and consequently efficiency of the inhibitor improved. It has been reported in our earlier contributions [9, 38] that the molecular band

gap is fundamentally more appropriate (than ΔE_{L-H}) to correlate experimentally determined inhibition properties of compounds. Furthermore, it has been reported that lower the ΔE_{MBS} of inhibitor, higher is the corrosion inhibition efficiency. Quantum chemical parameters presented in Table 5 confirmed good inhibition performance of albendazole as corrosion inhibitor and also confirmed strong interaction of albendazole molecules with the metal surface and thereby forming protective adsorption layer at mild steel/acid solution interface.

3.6. Mechanism of corrosion inhibition

Inhibition performance of Albendazole for mild steel/1 M HCl interface depends on the extent of adsorption and adsorption depends on several factors such as the number of adsorption sites, molecular size, and mode of interaction with the metal surface and extent of formation of metallic complexes. The adsorption of Albendazole at the mild steel surface can take place through its active centres; unshared electron pairs of hetero-atoms and pi-electron of the benzimidazole ring. In acidic solutions, it is known that inhibitor molecules can be protonated:



Thus in acid solution both neutral molecules and cationic forms of inhibitor exist [41]. It was assumed that Cl^- ion was first adsorbed onto the positively charged metal surface by coulombic attraction and then inhibitor molecules can be adsorbed through electrostatic interactions between the positively charged molecules and the negatively charged metal surface [41]. These adsorbed molecules interact with $(FeCl^-)_{ads}$ species to form monomolecular layers (by forming a complex) on the steel surface. These layers protect the mild steel surface from attack by chloride ions. Thus the oxidation of $(FeCl^-)_{ads}$ into Fe^{++} can be prevented. On the other hand, the protonated inhibitor molecules can also adsorb at cathodic sites in competition with hydrogen ions that going to reduce hydrogen evolution.

The neutral molecules may be adsorbed on the mild steel surface through the chemisorption mechanism, involving the displacement of water molecules from the mild steel surface and the sharing electrons between the hetero atoms and iron. The inhibitor molecules can also adsorb on the mild steel surface on the basis of donor-acceptor interactions between π -electrons of the aromatic ring and vacant d-orbitals of surface iron atoms.

4. CONCLUSIONS

a. Albendazole is a good inhibitor for the mild steel corrosion in 1 M HCl solution showing more than 90% inhibition efficiency at 0.4 mM Albendazole concentration. The results obtained from three different techniques viz., weight loss, EIS and polarization were in reasonably good agreement.

b. Electrochemical impedance measurements indicated that corrosion inhibition occurred by adsorption process. Tafel polarization curves show that the Albendazole acted as mixed-type inhibitor.

c. The adsorption of albendazole at mild steel/acid solution interface obeyed the Langmuir adsorption isotherm model and values of $\Delta G_{\text{ads}}^{\circ}$ indicated comprehensive adsorption mechanism.

d. Computed quantum chemical properties such as molecular band gap (ΔE_{MBG}), HOMO–LUMO energy gap ($\Delta E_{\text{L-H}}$) and E_{HOMO} and E_{LUMO} were found in good correlation with experimentally determined inhibition efficiency.

ACKNOWLEDGEMENTS

One of the authors Ishtiaque Ahamad wishes to acknowledge the Council of Science & Technology, Lucknow (UP) for providing grant under Young Scientist Scheme.

References

1. I. Ahamad, M.A. Quraishi, *Corros. Sci.* 51 (2009) 2006.
2. B. Hammouti, A. Aouniti, M. Taleb, M. Brighli, S. Kertit, *Corrosion* 51 (1995) 411.
3. A.Y. Musa, A.A.H. Kadhum, A.B. Mohamd, M.S. Takriff, A.R. Daud, S.K. Kamarudin, *Corros. Sci.* 52 (2010) 526.
4. S. Muralidharan, M.A. Quraishi, S.V.K. Iyer, *Corros. Sci.* 37 (1995) 1739.
5. H.B. Rudresh, S.M. Mayanna, *J. Electrochem. Soc.* 124 (1977) 340.
6. J.G.N. Thomas, Proc 5th Eur. Symp. Corrosion Inhibitors, Ann Univ Ferrara (1980) p. 453.
7. V.S. Sastri, J.R. Perumareddi, *Corrosion* 53 (1997) 617.
8. B. Gomez, N.V. Likhanova, M.A. Dominguez-Aguilar, R. Martinez-Palou, A. Vela, J.L. Gazquez, *J. Phys. Chem. B* 110 (2006) 8928.
9. I. Ahamad, R. Prasad, M.A. Quraishi, *Corros. Sci.* 52 (2010) 933.
10. G. Bereket, E. Hur, C. Ogretir, *J. Mol. Struct. (THEOCHEM)* 578 (2002) 79.
11. S.G. Zhang, W. Lei, M.Z. Xia, F.Y. Wang, *J. Mol. Struct. (THEOCHEM)* 732 (2005) 173.
12. S.K. Shukla, A.K. Singh, I. Ahamad, M.A. Quraishi, *Mater. Lett.* 63 (2009) 819.
13. I. Ahamad, M.A. Quraishi, *Corros. Sci.* 52 (2010) 651.
14. I. Ahamad, R. Prasad, M.A. Quraishi, *J. Solid State Electrochem.* 14 (2010) 2095.
15. I. Ahamad, R. Prasad, M.A. Quraishi, *Corros. Sci.* 52 (2010) 3033.
16. ASTM G1-3, Standard Practice for Preparing, Cleaning, and Evaluating Corrosion Test Specimens.
17. P.B. Mathur, T. Vasudevan, *Corrosion* 38 (1982) 171.
18. J.P. Perdew, K. Burke, M. Ernzerhof, *Phys. Rev. Lett.* 78 (1997) 1396.
19. L. Petit, P. Maldivi, C. Adamo, *J. Chem. Theory Comput.* 1 (2005) 953.
20. Gaussian 03, M.J. Frisch, G.W. Trucks, H.B. Schlegel, G.E. Scuseria, M.A. Robb, J.R. Cheeseman, J.A. Montgomery, Jr., T. Vreven, K. N. Kudin, J.C. Burant, J.M. Millam, S.S. Iyengar, J. Tomasi, V. Barone, B. Mennucci, M. Cossi, G. Scalmani, N. Rega, G.A. Petersson, H. Nakatsuji, M. Hada, M. Ehara, K. Toyota, R. Fukuda, J. Hasegawa, M. Ishida, T. Nakajima, Y. Honda, O. Kitao, H. Nakai, M. Klene, X. Li, J.E. Knox, H.P. Hratchian, J.B. Cross, V. Bakken, C. Adamo, J. Jaramillo, R. Gomperts, R.E. Stratmann, O. Yazyev, A.J. Austin, R. Cammi, C. Pomelli, J.W. Ochterski, P.Y. Ayala, K. Morokuma, G.A. Voth, P. Salvador, J.J. Dannenberg, V.G. Zakrzewski, S. Dapprich, A.D. Daniels, M.C. Strain, O. Farkas, D.K. Malick, A.D. Rabuck, K. Raghavachari, J.B. Foresman, J.V. Ortiz, Q. Cui, A.G. Baboul, S. Clifford, J. Cioslowski, B.B. Stefanov, G. Liu, A. Liashenko, P. Piskorz, I. Komaromi, R.L. Martin, D.J. Fox, T. Keith, M.A. Al-Laham, C.Y. Peng, A. Nanayakkara, M. Challacombe, P.M. W. Gill, B. Johnson, W. Chen, M.W. Wong, C. Gonzalez, and J.A. Pople, Gaussian, Inc., Wallingford CT, 2004.
21. Q.B. Zhang, Y.X. Hua, *Electrochim. Acta* 54 (2009) 1881.
22. E.A. Noor, A.H. Al-Moubaraki, *Mater. Chem. Phys.* 110 (2008) 145.

23. T. Szauer, A. Brandt, *Electrochim. Acta* 26 (1981) 1253.
24. L. Tang, G. Mu, G. Liu, *Corros. Sci.* 45 (2003) 2251.
25. K.J. Laidler, *Reaction Kinetics*, vol. 1, first ed. (1963) Pergmon Press, New York.
26. E. Cano, J.L. Polo, A. La Iglesia, J.M. Bastidas, *Adsorption* 10 (2004) 219.
27. G.K. Gomma, M.H. Wahdan, *Ind. J. Chem. Technol.* 2 (1995) 107.
28. M. Bouklah, B. Hammouti, M. Lagrenee, F. Bentiss, *Corros. Sci.* 48 (2006) 2831.
29. B.G. Ateya, B.E. El-Anadouli, F.M. El-Nizamy, *Corros. Sci.* 24 (1984) 497.
30. W. Li, Q. He, S. Zhang, C. Pei, B. Hou, *J. Appl. Electrochem.* 38 (2008) 289.
31. K. Juttner, *Electrochim. Acta* 35 (1990) 1501.
32. F. Mansfeld, *Corrosion* 36 (1981) 301.
33. A. Singh, I. Ahamad, V.K. Singh, M.A. Quraishi, *J. Solid State Electrochem.* 15 (2011) 1087.
34. C.S. Hsu, F. Mansfeld, *Corrosion* 57 (2001) 747.
35. E.E. Oguzie, Y. Li, F.H. Wang, *Electrochim. Acta* 53 (2007) 909.
36. A.A. Hermas, M.S. Morad, M.H. Wahdan, *J. Appl. Electrochem.* 34 (2004) 95.
37. I. Lukovits, E. Kalman, F. Zucchi, *Corrosion* 57 (2001) 3.
38. I. Ahamad, R. Prasad, M.A. Quraishi, *Corros. Sci.* 52 (2010) 1472.
39. J. Fang, J. Li, *J. Mol. Struct. (Theochem)* 593 (2002) 179.
40. P. Zhao, Q. Liang, Y. Li, *Appl. Surf. Sci.* 252 (2005) 1596.
41. M.A. Quraishi, M.Z.A. Rafiquee, S. Khan, N. Saxena, *J. Appl. Electrochem.* 37 (2007) 1153.